



Analysis of BDS GEO satellite multipath effect for GNSS integrity monitoring in civil aviation

Jin Chang¹ · Xingqun Zhan¹ · Yawei Zhai¹ · Shizhuang Wang¹ · Kui Lin¹

Received: 30 August 2020 / Revised: 8 November 2020 / Accepted: 10 November 2020
© The Author(s) 2021, corrected publication 2021

Abstract

With the great development of Global Navigation Satellite System (GNSS), multi-GNSS constellations (GPS, BDS, GLO-NASS, and Galileo) are able to provide users with more accurate positioning result. For civil aviation, to guarantee user's safety, multi-constellation GNSS needs to meet the integrity requirement. Using conservative error models, Multiple Hypothesis Solution Separation (MHSS) Advanced Receiver Autonomous Integrity Monitoring (ARAIM) is proposed to evaluate GNSS integrity. Current multipath error model in ARAIM algorithm is based on data of GPS Medium Earth Orbit (MEO) satellites. But BDS is a hybrid constellation. For BDS II, there has 5 Geosynchronous Earth Orbit (GEO) satellites. Previous studies have shown that the multipath effect of GEO satellites has statistical characteristics different from MEO satellites. Meanwhile, the multipath magnitude of GEO satellites is larger than that of MEO satellites. This paper mainly focuses on validating whether the multipath error model in ARAIM algorithm is conservative enough for GEO satellites. In this paper, Code Minus Carrier (CMC) residuals are calculated for BDS GEO dual-frequency signals. Then the Standard Deviation (STD) of CMC residuals can be conservatively estimated by bounded Cumulative Distribution Function (CDF). After eliminating interference from receiver noise, STD of GEO multipath can be obtained. Comparing the STD of GEO multipath effect with ARAIM multipath error model, a conclusion could be drawn that current multipath error model in ARAIM algorithm is no longer able to conservatively estimate the statistical characteristics of GEO satellites.

Keywords GNSS · Integrity · Multipath effect · Error model · GEO · BDS

1 Introduction

With the ability of providing positioning result worldwide, satellite-based navigation has been widely used in civil aviation. For civil aircraft, ensuring user's safety is of crucial significance. To guarantee the safety during the flight, International Civil Aviation Organization (ICAO) put forward four criteria to evaluate the performance of satellite-based navigation system: integrity, continuity, accuracy, availability [1]. Among them, two of the most challenging requirements for civil aviation are integrity and continuity [2]. Integrity is a measure of trust, which is used to determine whether the positioning results provided by navigation system is correct [3]. Continuity measures the ability of navigation system to operate without unplanned interruptions [1, 4].

✉ Xingqun Zhan
xqzhan@sjtu.edu.cn

¹ School of Aeronautics and Astronautics, Shanghai Jiao Tong University, Shanghai 200240, China

Before 2000s, Receiver Autonomous Integrity Monitoring (RAIM) had been developed to measure the integrity for civil aviation [5–7]. By checking the consistency of positioning residuals, RAIM becomes a supplemental navigation means for en-route through non-precision approach (NPA) phases of flight [8]. However, RAIM has a lot of drawbacks. One of the major drawbacks is occasional lack of availability [9]. With the navigation satellites increasing, using dual-frequency signals and multi-constellation positioning, MHSS ARAIM theory is proposed. MHSS ARAIM has better ability to provide integrity service. Many researchers have made great contributions to ARAIM user algorithm. Juan Blanch and Boris Pervan proposed Fault Detection (FD) scheme and Fault Exclusion (FE) scheme for ARAIM user algorithm [10, 11]. To determine the error magnitude of GPS satellite, Todd Walter analyzed GPS clock error as well as ephemeris error in detail and established the corresponding error model for these two errors [12]. In [13], Todd Walter specified two critical parameters for ARAIM user algorithm: the probability of satellite fault and the probability of constellation

fault. As for the multipath error model, Tim Murphy used GPS data from Boeing 777-300ER and 737-NG airplanes to build the STD-elevation error model [14].

BDS constellation is composed of MEO, Inclined Geosynchronous Orbit (IGSO) and GEO satellites. In Wide Area Augmentation System (WAAS), the ranging error of GEO satellites stands in a bias over a long time [15, 16] analyzed the fading characteristics of satellites in different orbits to explain this phenomenon. Gao et al. [16] shows that the orbit type of navigation satellites influences the multipath fading characteristic. As for GEO satellite in BDS II, [17] demonstrates that the multipath magnitude of BDS GEO satellites is larger than those of IGSO and MEO satellites. Moreover, the multipath effect is difficult to mitigate by increasing the observation period or averaging over multiple epochs [18]. Therefore, multipath error is one of error sources that could affect GNSS integrity. To determine the airframe multipath error model for GPS constellation, the initial model is proposed by [19] and [20] using the airframe multipath data. However, this model is shown to be insufficient [21]. Thus, the revised model is proposed by [22], which is also the current multipath error model for ARAIM algorithm. Current multipath error model in ARAIM user algorithm is based on GPS MEO satellite data. But this error model does not take BDS GEO satellites into consideration. When implementing GNSS integrity monitoring involving BDS constellation, the multipath error model of GEO needs to be determined.

To determine whether current multipath error model in ARAIM algorithm is conservative for BDS GEO satellites, this paper uses 24-h data with 1 Hz sample rate to validate the error model. The data is collected from chock ring antenna in Shanghai Jiao Tong University, which could mitigate the multipath effect. Meanwhile, comparing to the reflection of aircraft, since there are no obstacles around the antenna, the multipath magnitude of antenna is lower than that of aircraft. Code Minus Carrier (CMC) method is firstly used to calculate the margin of single frequency multipath residual. In this process, two methods are used to avoid cycle split effect. Due to ARAIM algorithm needs to conservatively guarantee user's safety [23], the worst-case scenario of multipath effect needs to be taken into account. Bounded CDF is used to determine the worst-case STD of multipath residual for BDS GEO satellites. However, the worst-case STD of multipath residual is contaminated by receiver noise. In the following step, the STD of receiver noise is analyzed using GNSS zero baseline data. After eliminating the interference of receiver noise, the multipath statistic characteristic of BDS GEO satellites can be obtained.

The paper is structured as follows. In the first part, the basic outline of MHSS based ARAIM user algorithm is given. The second part shows the method to calculate the

multipath residual. This part also introduces how to determine the conservative STD for multipath effect of BDS GEO satellites. After eliminating the interference of receiver noise, this part calculates statistic characteristic of multipath error. The last part is conclusion.

2 ARAIM background

2.1 ARAIM user algorithm

For satellite-based positioning, pseudorange positioning equation can be represented as

$$y = Hx + f + \epsilon \quad (1)$$

where H is a $n \times (3 + m)$ matrix. n is the number of pseudorange measurements and m is the number of constellations. x is a $(3 + m) \times 1$ vector, which includes the user's position and clock bias between different GNSS constellations. f is a $n \times 1$ vector, which indicates the fault magnitude in navigation system. ϵ is the noise vector, which includes the noise from satellite clock, ephemeris, troposphere, multipath and user's receiver. In order to calculate x , Weighted Least Square (WLS) method is used to solve Eq. (1):

$$\hat{x} = (H^T W H)^{-1} H^T W y \quad (2)$$

In (2), W is the weighted matrix, which is a diagonal matrix and can be derived from the error modes of ARAIM user algorithm. For SS ARAIM, we build N fault subsets to detect the possible faults which can severely affect GNSS accuracy. For detection function, positioning result of the i -th fault subset can be defined as

$$\hat{x}_i = (H^T W_i^{-1} H)^{-1} H^T W_i^{-1} y, i \in [1, N] \quad (3)$$

where W_i is calculated by weight matrix W after removing the measurements corresponding to the i th fault subset. Here gives an example of calculating W_i . Assuming the algorithm only monitors single satellite (the i th fault subset corresponds to the i th measurement) fault, W_i can be expressed as

$$\begin{cases} W_i(k, k) = W(k, k), k \neq i, k \in [1, N] \\ W_i(i, i) = 0 \end{cases} \quad (4)$$

To detect satellite fault in navigation system, detection statistic needs to be calculated. We define \hat{x}_0 as all in view positioning result, then the detection statistic can be calculated according to

$$\Delta_i = |\hat{x}_i - \hat{x}| \quad (5)$$

Based on the probability of false alert, the threshold T_i for different detection statistics can be determined. If $\Delta_i > T_i$, it means the fault has occurred in navigation system. To meet the continuity requirement of navigation system, fault exclusion function needs to be operated.

MHSS ARAIM builds N_1 sub-subsets to determine whether the exclusion function is implemented correctly. The positioning result of sub-subset can be expressed as

$$\hat{x}_{i,j} = \left(H^T W_{i,j}^{-1} H \right)^{-1} H^T W_{i,j}^{-1} y, \{j \in [1, N] | j \neq i\} \quad (6)$$

Here gives an example of calculating $W_{i,j}$. Assuming only single satellite fault is monitored by ARAIM algorithm, then both subset and sub-subset contain one satellite. If algorithm has detected GNSS fault. Fault exclusion function tries to exclude the faulty satellite to improve navigation performance. Firstly, FE algorithm chooses the satellite in the i th subset as the exclusion option. For a specific sub-subset j , $W_{i,j}$ can be denoted as

$$\begin{cases} W_{i,j}(k, k) = W(k, k), k \neq i, k \neq j \\ W_{i,j}(i, i) = 0 \\ W_{i,j}(j, j) = 0 \end{cases} \quad (7)$$

To measure the correctness of exclusion option, exclusion statistic needs to be calculated. Based on subset and sub-subset positioning result, the exclusion statistic can be calculated according to

$$\Delta_{i,j} = |\hat{x}_{i,j} - \hat{x}_i| \quad (8)$$

Using the probability of fault detection but not exclusion, the threshold $T_{ex,ij}$ for different exclusion statistics can be obtained. If exclusion option i is determined and $\forall \{j \in [1, N] | j \neq i\}$ meet $\Delta_{i,j} < T_{ex,ij}$, it represents the i th subset is the one that need to be excluded. Otherwise, the algorithm will change the exclusion option.

2.2 Error model of ARAIM

The error sources of GNSS can be divided into three types: (a) the error comes from satellite, which includes satellite clock and ephemeris error. (b) the error comes from signal propagation, which includes tropospheric and ionospheric error. (c) the error comes from user's environment, which includes multipath and receiver noise error.

To determine the statistic characteristics of these errors, [23] proposed corresponding error model to estimate the STD of them. For errors in (a), their STD can be measured by σ_{URE} . σ_{URE} can be obtained from broadcast ephemeris. The STD of tropospheric error σ_{tropo} in (b) can be measured by mode listed in (9) [24]. For MHSS ARAIM algorithm, it does not consider the ionospheric error, because the ionospheric error can be canceled

using dual frequency signals. For airborne GPS users, error models to determine the STD of error in (c) is well developed. The error models can be measured by (10), (11) and (12). In (10), f_{L1} and f_{L5} represent the signal frequency of GPS L1 and L5 signal. σ_{user} is the STD for airborne user error. σ_{MP} and σ_{noise} represent the STD of multipath and receiver noise, respectively:

$$\sigma_{tropo} = \frac{1.001}{\sqrt{0.002001 + \left(\sin\left(\frac{\pi\theta}{180}\right) \right)^2}} \quad (9)$$

$$\sigma_{user} = \frac{\sqrt{(f_{L1}^4 + f_{L5}^4)}}{f_{L1}^2 - f_{L5}^2} \sqrt{\sigma_{MP}^2 + \sigma_{noise}^2} \quad (10)$$

$$\sigma_{MP} = 0.13 + 0.53 \exp\left(-\frac{\theta}{10}\right) \quad (11)$$

$$\sigma_{noise} = 0.15 + 0.43 \exp\left(-\frac{\theta}{6.9}\right) \quad (12)$$

For every GNSS satellite, the Eq. (9), (10) and σ_{URE} can derive the weight matrix that used for WLS method to solve (1). The weight matrix can be expressed as

$$W = \begin{bmatrix} \sigma_1^2 & \dots & 0 \\ \vdots & \ddots & \vdots \\ 0 & \dots & \sigma_n^2 \end{bmatrix}^{-1} \quad (13)$$

where $\sigma_i^2 = \sigma_{URE,i}^2 + \sigma_{tropo,i}^2 + \sigma_{user,i}^2$, the subscript i represents the i -th diagonal element of W .

3 The calculation of multipath variance

3.1 Code minus carrier method

For GNSS receiver, multipath delay results in tracking error of code correlator. The tracking error causes GNSS receiver to generate faulty code and carrier phase measurement. Multipath effect can severely affect the magnitude of code measurement, because the wavelength of carrier phase is much smaller than chip interval [25]. According to this property, multipath residuals for different GNSS signal frequencies can be calculated through the combinations of code measurement and carrier phase measurement in (14) and (15) [18, 18, 18]:

$$MP_{f_1} = PR_{f_1} - \frac{f_1^2 + f_2^2}{f_1^2 - f_2^2} \phi_{f_1} \lambda_{f_1} + \frac{2f_2^2}{f_1^2 - f_2^2} \phi_{f_2} \lambda_{f_2} - N_{f_1} + \epsilon \quad (14)$$

$$MP_{f_2} = PR_{f_2} + \frac{f_1^2 + f_2^2}{f_1^2 - f_2^2} \phi_{f_2} \lambda_{f_2} - \frac{2f_1^2}{f_1^2 - f_2^2} \phi_{f_1} \lambda_{f_1} - N_{f_2} + \epsilon \quad (15)$$

In (14) and (15), MP_{f_1} and MP_{f_2} are multipath residuals of frequency f_1 and f_2 , respectively. N_{f_1} and N_{f_2} are integer ambiguities which can be seemed as constant bias when there is no cycle slip occurs [26]. λ_1 and λ_2 are the wavelength of GNSS signal at f_1 and f_2 frequency, respectively. ϵ is GNSS receiver noise. Actually, the residuals in (14) and (15) contain the integer ambiguities which needs to be eliminated.

3.2 Cycle slip detection and repairation

Before eliminating the constant term in (14) and (15), the effect of cycle slip needs to be avoided. Based on [28], we combine Total Electron Contents Rate (TECR) and Melbourne–Wübbena wide-lane (MWWL) method to detect and repair the cycle slip.

Assume that the ionospheric delay changes very slowly with time. Test statistic can be derived from ionospheric residual from epoch k and epoch $k - 1$. (16) is the equation to calculate TECR test statistic. In (16), $\phi_{1,k}$ is carrier phase observation of f_1 frequency signal at epoch k . $\phi_{2,k}$ is the carrier phase observation of f_2 frequency signal at epoch $k - 1$. According to the law of error propagation, the threshold $T_{TECR,k}$ of $\Delta_{TECR,k}$ is set to 0.07 [29]. (17) is the equation that can be used to calculate the cycle split magnitude $\Delta N_{1,k}$ and $\Delta N_{2,k}$ at frequency f_1 and f_2 at epoch k :

$$\Delta_{TECR,k} = \phi_{1,k} - \frac{f_1}{f_2}\phi_{2,k} - \phi_{1,k-1} + \frac{f_1}{f_2}\phi_{2,k-1} \quad (16)$$

$$\Delta_{TECR,k} = \Delta N_{1,k} - \frac{f_1}{f_2}\Delta N_{2,k} \quad (17)$$

TECR has its own drawback. When $\lambda_1\Delta N_{1,k} = \lambda_2\Delta N_{2,k}$, TECR cannot detect the cycle split. To solve this problem and repair the cycle split. MWWL test statistic $\Delta_{MWWL,k}$ is introduced [29]:

$$L_{MWWL,k} = (\phi_{1,k} - \phi_{2,k}) - \frac{f_1 - f_2}{f_1 + f_2} \left(\frac{PR_{1,k}}{\lambda_1} + \frac{PR_{2,k}}{\lambda_2} \right) \quad (18)$$

$$\Delta_{MWWL,k} = L_{MWWL,k} - L_{MWWL,k-1} \quad (19)$$

$$\Delta_{MWWL,k} = \Delta N_{1,k} - \Delta N_{2,k} \quad (20)$$

In (18), $PR_{1,k}$ is pseudorange measurement of frequency f_1 at epoch k . $PR_{2,k}$ is pseudorange measurement of frequency f_2 at epoch k . The threshold $T_{MWWL,k}$ of test statistic $\Delta_{MWWL,k}$ is set to 1 based on [29]. (20) can be used to calculate the cycle split magnitude $\Delta N_{1,k}$ and $\Delta N_{2,k}$ at frequency f_1 and f_2 at epoch k .

If $|\Delta_{MWWL,k}| > T_{MWWL,k}$ or $|\Delta_{TECR,k}| > T_{TECR,k}$, the cycle split is detected. Then, combining (17) and (20), the magnitude of cycle split can be obtained. To validate the effectiveness of this method, we first select 200 s GNSS

observation data from BDS GEO 01 satellite which is not affected by cycle slip. Figure 1 shows the magnitude of TECR and MWWL test statistic.

Assuming that B1 frequency carrier phase observations are affected by cycle slip at 100 s. The magnitude of cycle slip is set to 100 cycle. Figure 2 shows the result of TECR and MWWL test statistic.

In Fig. 2, both TECR and MWWL method can detect the cycle slip. Based on (17) and (20), the magnitude of cycle slip in B1 and B2 frequencies can be expressed as follows:

$$\Delta N_{1,k} = \left[\frac{f_1}{f_2 - f_1} \left(\frac{f_2}{f_1} \Delta_{TECR,k} - \Delta_{MWWL,k} \right) \right] \quad (21)$$

$$\Delta N_{2,k} = \left[\frac{f_2}{f_2 - f_1} \left(\Delta_{TECR,k} - \Delta_{MWWL,k} \right) \right] \quad (22)$$

where [] represents the rounding process. Because the magnitude of cycle slip can only be integer, the repair results of cycle slip need to be rounded. In this case, the repair results are 99 cycle and 1 cycle for B1 and B2 frequency, respectively. The results show that the method can effectively repair the cycle slip.

3.3 Multipath residual calculation

After removing the cycle split effect from carrier phase measurement, the constant term in (14) and (15) can be eliminated. The multipath residual can be calculated according to:

$$MP_{f_i,r}(n) = MP_{f_i}(n) - \frac{1}{m} \sum_{k=1}^m MP_{f_i}(k) \quad (23)$$

where $MP_{f_i,r}(n)$ is multipath residual of frequency f_i at epoch n . $MP_{f_i}(n)$ is multipath residual of frequency f_i at epoch n and contains the integer ambiguities. m is the number of MP_{f_i} .

3.4 Receiver noise estimation using zero baseline test

In (23), the multipath residual still contains the receiver noise. To remove the interference of receiver noise, GNSS zero baseline data is used to estimate the receiver noise. Zero baseline test is a method to assess the intrinsic noise characteristics of GNSS receiver [30]. The test requires two receivers of the same type. Two receivers need to connect to the same antenna. The experiment environment is shown in Fig. 3.

The pseudorange of receiver a and b can be expressed in (24) and (25):

$$PR_i^a = |x_{\text{sat}} - x_{\text{pos}}| + c\delta_t^a + \delta_{\text{tropo}} + \delta_{\text{ion}} + \delta_{\text{MP}} + \epsilon \quad (24)$$

Fig. 1 TECR and MWWL test statistic magnitude without cycle slip

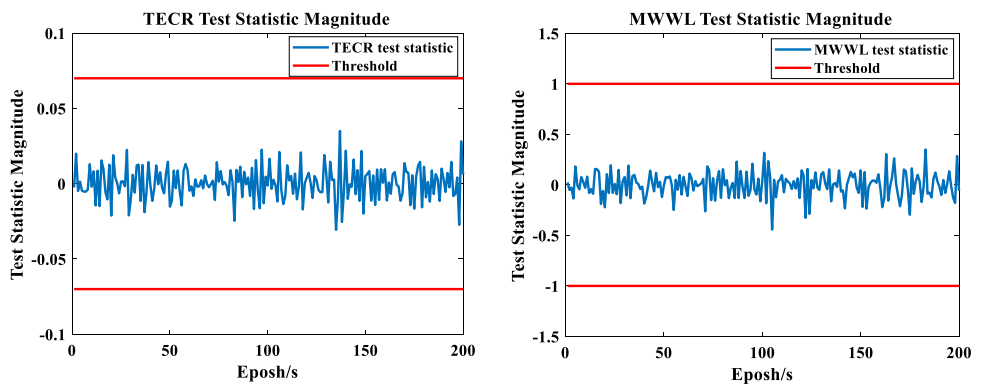


Fig. 2 TECR and MWWL test statistic magnitude with cycle slip

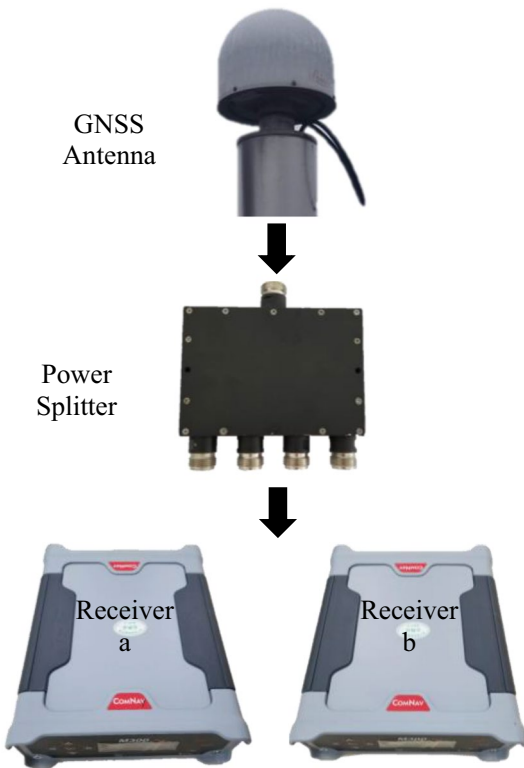
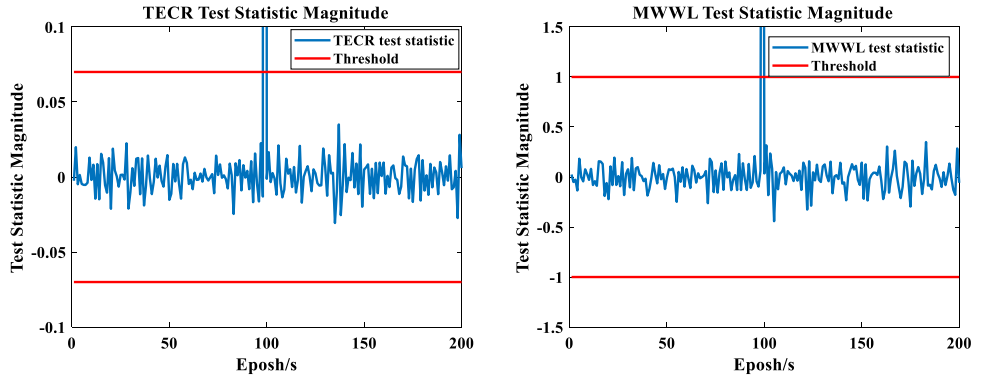


Fig. 3 Experiment environment of zero baseline test

$$PR_i^b = |\mathbf{x}_{\text{sat}} - \mathbf{x}_{\text{pos}}| + c\delta_t^b + \delta_{\text{tropo}} + \delta_{\text{ion}} + \delta_{\text{MP}} + \epsilon \quad (25)$$

where the superscript a and b represent different receivers in zero baseline test. c is the speed of light. x_{sat} and x_{pos} represent the position of satellite and antenna. δ_t , δ_{tropo} , δ_{ion} and δ_{MP} are receiver clock bias, tropospheric error, ionospheric error and multipath error. By Subtracting (25) from (24), Single Difference (SD) result ΔPR_i^{ba} is obtained:

$$\Delta PR_i^{ba} = PR_i^a - PR_i^b = c(\delta_{tb} - \delta_{ta}) + \epsilon_{\text{SD}} \quad (26)$$

ϵ_{SD} is receiver noise of SD result. In SD result, external errors such as atmospheric errors, satellite-dependent errors and multipath can be canceled. Receiver noise and clock bias are the only two errors in SD result.

Since SD result is affected by clock bias, DD residual $\nabla \Delta PR_i^{ba}$ which only contains receiver noise can be represented by (27). The subscript j is the reference satellite with high Carrier to Noise Ratio (CNR). ϵ_{DD} is receiver noise of DD result.

$$\nabla \Delta PR_i^{ba} = \Delta PR_i^{ba} - \Delta PR_j^{ba} = \epsilon_{\text{DD}} \quad (27)$$

Time series of receiver noise for different satellite can be obtained from DD residual. However, the DD residual of the reference satellites cannot be obtained. Therefore, based on [31], this paper uses DD result to recover SD sequence which is not affected by receiver clock bias. Assuming that

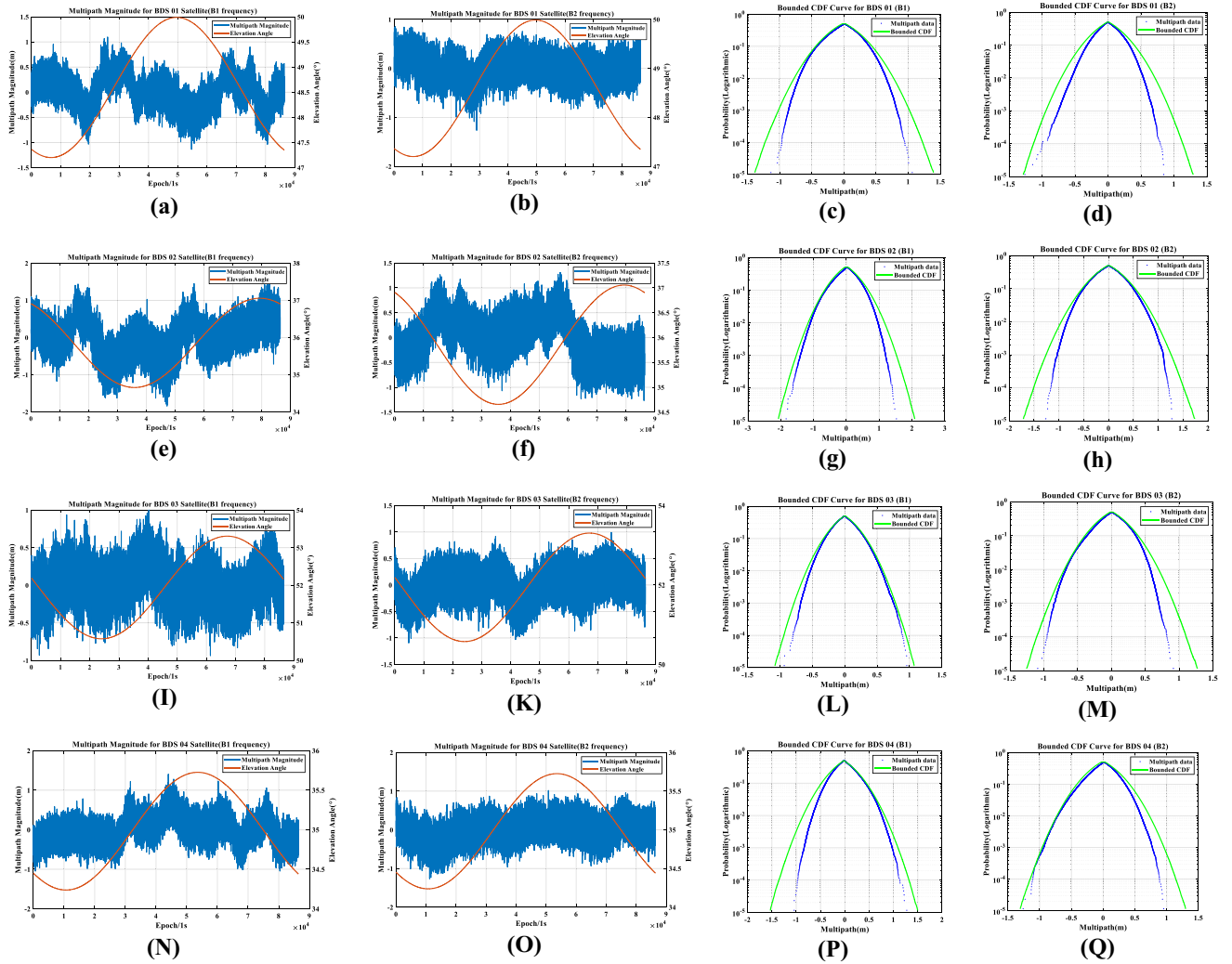


Fig. 4 Multipath Residual Result and bounding process

the first satellite is reference satellite, DD sequences can be expressed as

$$\left\{ \begin{array}{l} \epsilon_{DD,12} = \epsilon_{SD,1} - \epsilon_{SD,2} \\ \epsilon_{DD,13} = \epsilon_{SD,1} - \epsilon_{SD,3} \\ \dots \\ \epsilon_{DD,1i} = \epsilon_{SD,1} - \epsilon_{SD,i} \\ \dots \\ \epsilon_{DD,1n} = \epsilon_{SD,1} - \epsilon_{SD,n} \end{array} \right. \quad (28)$$

where the subscript $1i$ represents the DD residual between the first and the i th satellite. The subscript of i represents the i th satellite. Since GNSS intrinsic receiver noise is Gaussian white noise, the sum of SD sequence obeys Gaussian

distribution with zero bias. Using this character and solving (29), SD sequence can be obtained:

$$\begin{bmatrix} \epsilon_{DD,12} \\ b\epsilon_{DD,13} \\ \dots \\ \epsilon_{DD,1n} \\ 0 \end{bmatrix} = \begin{bmatrix} 1 & -1 & 0 & \dots & 0 \\ 1 & 0 & -1 & \dots & 0 \\ \dots & \dots & \dots & \dots & \dots \\ 1 & 0 & 0 & \dots & -1 \\ 1 & 1 & 1 & \dots & 1 \end{bmatrix} \begin{bmatrix} \epsilon_{SD,1} \\ \epsilon_{SD,2} \\ \dots \\ \epsilon_{SD,n-1} \\ \epsilon_{SD,n} \end{bmatrix} \quad (29)$$

After bounding SD sequence and multipath residual, the statistic characteristic of BDS II GEO multipath can be calculated. By comparing with STD calculated from ARAIM model, this paper examines whether ARAIM multipath model could be used for BDS GEO satellite.

Table 1 Standard deviation of multipath residual

σ_{MR} GEO	B1(STD/m)	B2(STD/m)
BDS 01	0.3015	0.3215
BDS 02	0.4801	0.4001
BDS 03	0.2506	0.2906
BDS 04	0.3600	0.3113

Table 2 Standard deviation of SD sequence

σ_{SD} GEO	B1(STD/m)	B2(STD/m)
BDS 01	0.2185	0.1600
BDS 02	0.3150	0.1985
BDS 03	0.2485	0.1994
BDS 04	0.2590	0.2050

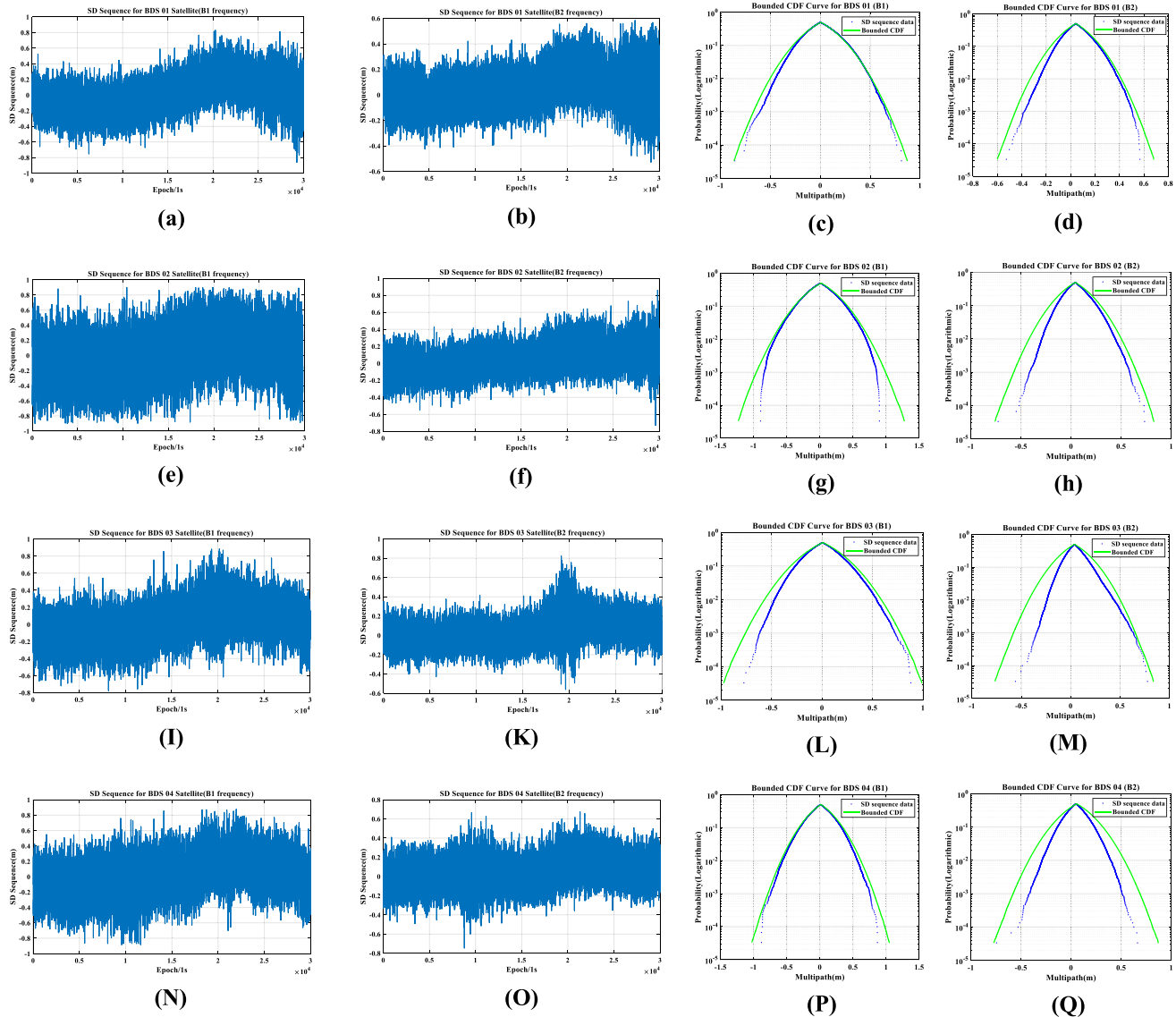
**Fig. 5** Receiver Noise result and bounding process

Table 3 Standard deviation of multipath magnitude

σ_{MP} GEO	B1(STD/m)	B2(STD/m)
BDS 01	0.2589	0.3009
BDS 02	0.4253	0.3747
BDS 03	0.2485	0.2541
BDS 04	0.2590	0.2755

4 Experiment result

4.1 Multipath residual for BDS GEO satellite

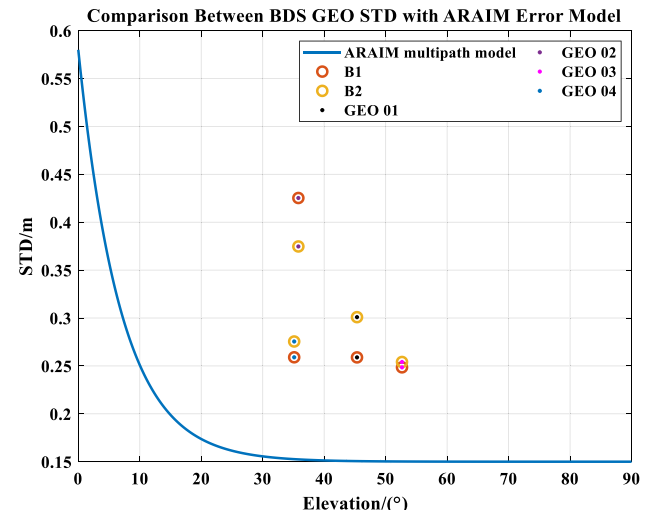
24-h data is used to calculate the multipath residual of BDS GEO satellites. The STD of multipath residual can be conservatively estimated by bounding process. Due to the low elevation angle, the signal from BDS 05 satellite is highly susceptible to the interference. So, in this paper, we only analyze four BDS II GEO satellites.

Table 1 shows the bounded STD value σ_{MR} of BDS 01 to 04 satellite at different frequencies (B1 and B2 frequency). Figure 4 shows the multipath residual and bounding results. Take BDS 01 satellite as an example, Figure 4a, b show the variation of multipath residual and elevation over time. The orange line and blue line represent the elevation angle and multipath residual. Figure 4c,d shows the bounding results, the blue dot represents the folded CDF of multipath residual data. The green line is the bounded CDF, which can conservatively estimate the STD of multipath residual data.

4.2 SD sequence for BDS GEO satellite

Even the STD of multipath residual can be obtained, the result still affected by receiver noise. To eliminate the interference of receiver noise, receiver noise evaluation is implemented. For receiver noise evaluation, this paper uses 8-h data to obtain SD sequence for different GEO satellites. This paper only analyzes the receiver noise for BDS 01 to 04.

Table 2 shows the bounded STD value σ_{SD} of SD sequence at different frequencies (B1 and B2 frequency). Figure 5 shows the time series of GNSS receiver noise. At the same time, Fig. 5 also shows the bounding result of receiver noise for different BDS GEO satellite at difference frequencies. Take GEO 01 satellite as an example, Fig. 5a, b shows the SD sequence result of receiver noise. Figure 5c, d shows the bounding results which can conservatively estimate the STD of SD sequence.

**Fig. 6** Comparison between BDS GEO STD ARAIM error model

4.3 Multipath magnitude evaluation for BDS GEO satellite

Based on previous analysis in this paper, multipath residual is affected by receiver noise. Therefore, the STD of multipath residual σ_{MR} can be expressed as

$$\sigma_{MR} = \sqrt{\sigma_{MP}^2 + \sigma_{noise}^2} \quad (30)$$

where σ_{noise} is receiver noise.

Based on (30), the STD of multipath can be obtained by following:

$$\sigma_{MP} = \sqrt{\sigma_{MR}^2 - \sigma_{noise}^2} \quad (31)$$

The relationship between the STD of SD result and σ_{noise} can be described as

$$\sigma_{SD} = \sqrt{2}\sigma_{noise} \quad (32)$$

where σ_{SD} can be obtained from Table 2. Using (30), (31) and (32), σ_{MP} for BDS GEO 01 to 04 is shown in Table 3.

Figure 6 shows the difference of STD between ARAIM model and BDS GEO satellites. The circles in Fig. 6 represents different frequencies of BDS. The dots with different color in the circle represent different GEO satellites.

As shown in Fig. 6, whether at B1 or B2 frequency, the STD values of BDS GEO satellites are far larger than ARAIM error model.

5 Conclusions

This work investigated whether the multipath error model in ARAIM algorithm is suitable for BDS II GEO satellites. This paper firstly calculates the multipath residual using CMC method. In this step, to avoid the interference of cycle slip, TECR and MWWL method is used to detect and repair the cycle slip. Since the results of multipath residual are contaminated by receiver noise, GNSS zero baseline data is used to estimate the receiver noise. After eliminating the interference of receiver noise, we conservatively estimate the STD of multipath residual for BDS II GEO satellites. We find that the error model in ARAIM user algorithm are not suitable for BDS II GEO satellites. In the future, for GNSS integrity monitoring system using BDS II GEO satellites, the multipath error model of these satellites should be refined.

Open Access This article is licensed under a Creative Commons Attribution 4.0 International License, which permits use, sharing, adaptation, distribution and reproduction in any medium or format, as long as you give appropriate credit to the original author(s) and the source, provide a link to the Creative Commons licence, and indicate if changes were made. The images or other third party material in this article are included in the article's Creative Commons licence, unless indicated otherwise in a credit line to the material. If material is not included in the article's Creative Commons licence and your intended use is not permitted by statutory regulation or exceeds the permitted use, you will need to obtain permission directly from the copyright holder. To view a copy of this licence, visit <http://creativecommons.org/licenses/by/4.0/>.

References

- International Civil Aviation Organization (ICAO), Annex 10: Aeronautical Telecommunications. Volume 1: (Radio Navigation Aids), Amendment 84, published 20 July.
- Zhai YW (2018) Ensuring navigation integrity and continuity using multi-constellation GNSS, PhD. Dissertation, Illinois Institute of Technology, Chicago, IL.
- Zhai YW, Zhan XQ, Chang J, Pervan B (2019) ARAIM with More than two constellations, ION 2019 Pacific PNT Meeting, pp 925–941. <https://doi.org/10.33012/2019.16849>
- Zhai YW, Zhan XQ, Joerger M, Pervan B (2018) Impact quantification of satellite outages on air navigation continuity. IET Radar Sonar Navig. <https://doi.org/10.1049/iet-rsn.2018.5376>
- Lee YC (1999) Analysis of range and position comparison methods as a means to provide gps integrity in the user receiver. In: Proceedings of the annual meeting of the institute of navigation.
- Parkinson B, Axelrad P (1988) Autonomous GPS integrity monitoring using the pseudorange residual. Navigation. <https://doi.org/10.1002/j.2161-4296.1988.tb00955.x>
- Brown G, Hwang P (1986) GPS failure detection by autonomous means within the cockpit. Navigation 33:335–353. <https://doi.org/10.1002/j.2161-4296.1986.tb01485.x>
- Yang YX, Xu JY (2016) GNSS receiver autonomous integrity monitoring (RAIM) algorithm based on robust estimation. Geodesy Geodyn. <https://doi.org/10.1016/j.geog.2016.04.004>
- Hwang P, Brown R (2006) RAIM-FDE revisited: a new breakthrough in availability performance with NIORAIM (novel integrity-optimized RAIM). Navigation 53:41–51. <https://doi.org/10.1002/j.2161-4296.2006.tb00370.x>
- Blanch J, Walter T, Enge P, Wallner S, Fernandez F, Dellago R, Ioannides R, Pervan B, Fernandez-Hernandez I, Belabbas B, Spletter A, Rippl M (2011) A proposal for multi-constellation advanced raim for vertical guidance. In: International Technical Meeting of the Satellite Division of The Institute of Navigation.
- Joerger M, Pervan B (2016) Fault detection and exclusion using solution separation and chi-squared ARAIM. IEEE Trans Aerosp Electron Syst 52:726–742. <https://doi.org/10.1109/TAES.2015.140589>
- Walter T, Blanch J (2015) Characterization of GNSS Clock and Ephemeris Errors to Support ARAIM. Proceedings of the ION 2015 Pacific PNT Meeting, Honolulu, Hawaii, pp. 920–931.
- Walter T, Blanch J, Joerger M, Pervan B (2016) Determination of fault probabilities for ARAIM. IEEE/ION position location and navigation symposium(PLANS). <https://doi.org/10.1109/PLANS.2016.7479733>
- Murphy T, Friedman R, Booth J, Geren P, Molloy N, Clark B, Burns J (2004) Program for the investigation of airborne multipath errors 2004: 781–792
- Schempp T, Burke J, Rubin A (2008) WAAS benefits of GEO ranging. International Technical Meeting of the Satellite Division of the Institute of Navigation, ION GNSS (Vol. 4, pp. 2000–2007).
- Gao Y, Cui XW, Lu MG, Li H, Feng ZM (2012) The analysis and simulation of multipath error fading characterization in different satellite orbits. https://doi.org/10.1007/978-3-642-29193-7_29
- Zhang F, He H, Tang B (2013) Analysis of signal characteristic and positioning performance affected by pseudorange multipath for COMPASS. China Satellite Navig Conf (CSNC). https://doi.org/10.1007/978-3-642-37398-5_45
- Wang G, De JK, Zhao Q (2015) Multipath analysis of code measurements for BeiDou geostationary satellites. GPS Solut 19(1):129–139
- McGraw G (2000) Derivation of LAAS Pseudorange Accuracy Allocations (1998) Presented as Working Paper 59 from GNSSP/WG B meeting.
- Murph T, Snow R, Braasch M (1996) GPS multipath of air transport airframes. The Journal of the Institute of Navigation, Navigation, pp. 397–406.
- McGraw G, Murphy T, Brenner M, Pullen S, Van Dierendonck AJ (2000) Development of the LAAS Accuracy Models. In: Proceedings of the 13th International Technical Meeting of the Satellite Division of The Institute of Navigation, pp. 1212–1223.
- Murphy T, Booth J (2000) GBAS SARPs Review and Validation of Airborne Multipath Requirements. GNSSP WG B.
- EU-U.S. Cooperation on Satellite Navigation, Working Group C, ARAIM Technical Subgroup Milestone 3Report. February 25, 2016.
- United States Federal Aviation Administration (1992) Aircraft certification service airborne supplemental navigation equipment using the global positioning system (GPS). Aircraft Certification Service, Washington, D.C.
- Fang CH, Lan XQ, Xiang RR (2016) Cycle slip detection and reparation for dual frequency GPS data by integrating Two Methods. J Site Investig Sci Technol 04:22–25
- El-Rabbany, A (2002) Introduction to GPS: the global positioning system. Artech house.
- Shi C, Zhao Q, Hu Z (2013) Precise relative positioning using real tracking data from COMPASS GEO and IGSO satellites. GPS Solut 17(1):103–119
- Wanninger L, Beer S (2015) BeiDou satellite-induced code pseudorange variations: diagnosis and therapy. GPS Solut. <https://doi.org/10.1007/s10291-014-0423-3>

-
- 29. Liu ZZ (2011) A new automated cycle slip detection and repair method for a single dual-frequency GPS receiver. *J Geodesy* 85(3):171–183
 - 30. Amiri-Simkooei AR, Tiberius CCJM (2007) Assessing receiver noise using GPS short baseline time series. *GPS Solut* 11(1):21–35
 - 31. Li JL, Ma JF, Fu JY (2016) Principle analysis of deriving single-differenced residuals from double-differenced residuals in GNSS data processing. *J Geom Technol* 33(01):1–5